Jana, S., A. Gangopadhyay, P.F.J. Lermusiaux, A. Chakraborty, and P.J. Haley, Jr., 2024. Impact of River Inputs on Sound Speed Structures in the Bay of Bengal. In: OCEANS '24 IEEE/MTS Singapore, 14–18 April 2024, in press.

Impact of River Inputs on Sound Speed Structures in the Bay of Bengal

1st Sudip Jana
Department of Mathematics
Adamas University
Kolkata, India
sudip.ocn@gmail.com

2nd Avijit Gangopadhyay
School for Marine Science and Technology
University of Massachusetts Dartmouth
Dartmouth, MA, USA
avijit.gangopadhyay@umassd.edu

3rd Pierre F. J. Lermusiaux
Department of Mechanical Engineering
Massachusetts Institute of Technology
Cambridge, MA, USA
pierrel@mit.edu

4th Arun Chakraborty
Centre for Ocean, River, Atmosphere and Land Sciences
Indian Institute of Technology Kharagpur
Kharagpur, India
arunc@coral.iitkgp.ac.in

5th Patrick J. Haley, Jr.
Department of Mechanical Engineering
Massachusetts Institute of Technology
Cambridge, MA, USA
phaley@mit.edu

***Abstract*—The Bay of Bengal (BoB) exhibits a distinctive pattern of surface freshening primarily resulting from runoff originating from several major rivers and the monsoon precipitation. This freshening significantly modulates the spatial and temporal variations in the thermohaline structure, ultimately shaping the sound speed structure within this region. This study investigates the seasonal impact of river input on the sound speed structure of the BoB through two numerical simulations with and without river input using the Regional Ocean Modeling System (ROMS). The findings indicate that river inputs consistently reduce the surface sound speed across the domain throughout the year, with the most noticeable effect occurring in the northern part of BoB during the post-monsoon months of October and November. During this period, the surface variability is predominately driven by salinity variations induced by river inputs. In contrast, in the subsurface layers, the influence of reduced salinity becomes less pronounced with increasing depth, and the temperature modulations brought about by river inputs play a more important role. Freshening in the surface layers leads to the creation of a stratified barrier layer just below the mixed layer. Consequently, this results in the formation of warm temperature inversions in the subsurface layers, with cooling occurring beneath them. These phenomena contribute to variations in the sound speed, causing it to increase within the inversion layer and decrease below it. Notably, the sonic layer depth (SLD) is found to become shallower in the presence of river inputs during the post-monsoon and winter seasons in the northern BoB. The combination of enhanced vertical salinity gradients and subsurface temperature inversions significantly amplifies the vertical gradient of sound speed above the SLD. This, in turn, may lead to the development of more robust surface ducts and the expansion of shadow zones beneath the SLD.**

Keywords—Sound speed variability, Bay of Bengal, River inputs, ROMS, Sonic layer depth, Surface duct

I. INTRODUCTION

Understanding the underwater acoustic environment is crucial for various scientific and strategic applications, ranging from oceanographic research to naval operations. Sound speed is a critical factor in acoustic propagation that is used for underwater communication, sonar systems, and monitoring of ocean interiors and processes. Sound speed within the ocean depends on three major parameters - temperature, salinity, and pressure [1]-[3]. Therefore, the distribution of sound speed in the ocean varies within a region with seasons and with changes in the thermohaline structures due to water-mass circulation. While temperature generally has a significantly greater impact [4] on sound speed variability than salinity, the latter becomes crucial in regions of high salinity contrast [5]. The Bay of Bengal (BoB) (Fig. 1) is one such region exhibiting large spatiotemporal contrasts in salinity. This is attributed to the vast influx of freshwater from the monsoon rain and the runoff from several rivers in the surrounding countries [6-14]. The massive runoff from the Ganges-Brahmaputra-Meghna (GBM) River system, coupled with other rivers makes the northern BoB the most freshwater-rich area of the tropical global ocean. This freshwater spreads over the BoB in the form of freshwater pools, plumes, and filaments. These features can greatly influence the thermohaline structure through the formation of haline stratification, barrier layer, and temperature inversion [11], [13], [15]-[18], all of which modify the sound speed structure.

There are a few studies in the literature that addressed the sound speed structure and variability in the BoB. In one such study, through a comparative analysis, [19] showed that the spatial variation of sound speed in BoB is lesser than in the Arabian Sea (AS). In [20], the authors showed the effect of cold-core eddies on acoustic propagation in the BoB. Using observational data along the west coast of Andaman Island, [21] found that the sound speed gradient showed better agreement with the temperature gradient than the salinity gradient. Using Glider data [22] highlighted the formation of afternoon effects in the sound speed profile and of a secondary sound channel in the central BoB. In [23], the authors identified the role of the salinity variability due to river discharge in acoustic reflection. They studied seismic data near the Krishna-Godavari River mouth and showed that the salinity effect cannot be ignored in

modeling the acoustic reflection. Recently, using ten years of Argo data, [24] studied the upper ocean sound speed structure and variability over the BoB. They showed the domain-wide as well as region-specific variability and identified the effect of the extreme surface freshening on the higher sound speed variability in the northern BoB.

Multiple studies investigated the impact of river input on the Bay of Bengal using different numerical models [8]-[14]. These studies were mostly concerned with the effect of river runoff on the thermohaline structure and the ocean dynamics. However, the impact of rivers on the sound speed has not been studied yet.

In this study, we investigate the role of river inputs on the sound speed structure and variability over the Bay of Bengal by utilizing the modeling system set up by [12], [14]. The paper is organized as follows. Section II describes the modeling system setup and method of computing sound speed. Section III presents the results of the river input impact on the sound speed structure. Section IV summarizes the study by highlighting the major findings.

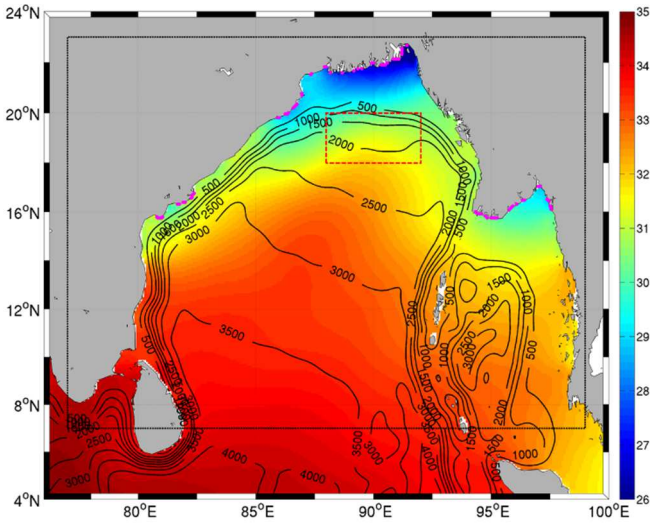

Fig. 1. The model domain with WOA01 climatological annual salinity (shaded background). Contours represent the model bathymetry values. Magenta points along the boundary are the location of the point sources. The dotted red box in the northern BoB represents the area to obtain averaged vertical profiles of temperature, salinity, and sound speed.

II. Model and Method

A. Modeling System Setup

In this study, we investigate the impact of river inputs on the structure and variability of the sound speed field over the BoB region using the Regional Ocean Modeling System (ROMS) [25]-[27]. The modeling system setup used is based on those of [12], [14]. The ROMS was configured over a domain (Fig. 1) that extends from 76°E to 100°E and from 4°N to 24°N, with a uniform horizontal resolution of 1/12° (~9 km) and 32 terrain-following vertical layers. River inputs are integrated into the model as point sources, situated near the river mouths on the model's coastal boundary. The seasonal river inputs represent the average monthly discharges from ten major rivers: Krishna, Godavari, Mahanadi, Brahmani, Subarnarekha, Hooghly, Ganges-Brahmaputra-Meghna (GBM), Irrawaddy, Sittang, and Salween. The seasonal cycles of discharges from all these rivers were provided in Figure 2 of [12].

The monthly climatological forcing fields consist of (i) 0.25°QuikSCAT wind stress [28]; (ii) net longwave and shortwave radiations from OAFlux product Project [29], [30] acquired from the International Satellite Cloud Climatology Project (ISCCP); (iii) precipitation from CORE 2 (Coordinated Ocean Research Experiments version 2) [31] datasets; and (iv) air temperature, air density, relative humidity, and specific humidity from the 0.5° COADS monthly climatology [32]. The latent and sensible heat fluxes and evaporation were calculated within the model using the bulk formula [33]. Figure 2d shows the seasonal cycles of the river discharges from all the rivers. Extensive validations of modeling system setup and simulations were carried out on the temperature, salinity, and currents in [12].

Two parallel climatological mesoscale simulations were carried out for fifteen years: one without any river input, called No River Run (NoRR), and the other including the river inputs, called the River Run (RR). The simulated fields of the last five years were used to obtain monthly climatological fields for further analysis.

B. Computation of Sound Speed

The sound speed fields were computed from the model-simulated temperature and salinity fields using Medwin's formula [1]:

$$C = 1449.2 + 4.6T - 0.055T^2 + 0.00029T^3 + (1.34 - 0.01T)(S - 35) + 0.016Z$$

where T is the temperature (°C), S the salinity (ppt) and Z the depth (m).

III. Results and Discussion

A. Impact on Surface Variability

Figure 2 compares the annual mean sound speed fields from the NIOA [34], RR, and NoRR at the surface. The RR sound speed shows good agreement with that from the climatology. On an annual scale, the sound speed is lowest at the northern end and gradually increases towards the south and southwest. The NoRR sound speed map shows a somewhat similar pattern, but the values are significantly higher than the RR field. The difference field in Fig 2(d) quantifies the impact of river input on the annual sound speed. The river input reduces the sound speed throughout the domain.

Figure 3 demonstrates the seasonal variability of the river impact on the domain-wide surface sound speed in terms of domain-averaged mean and spatial standard deviation. The spatial standard deviation quantifies the intensity/amount of the spatial variability. The seasonal variability of the domain-averaged sound speed (Fig. 3a) in both simulations follows the same pattern as that of the temperature. This indicates the dominant impact of temperature in determining the seasonal variability in domain-wide sound speed. However, the river input reduces the domain-averaged sound speed throughout the

year by ~1-2 m/s. These range values are much higher at the northern end of the Bay as evident in Fig. 2 and Fig. 4. The intensity of the sound speed reduction due to river input is the lowest during the pre-monsoon period (when the river discharge and surface freshening are minimum) and increases gradually as the monsoon progresses and freshwater supply from rivers increases and reaches to a peak in October. This is because, while during October the river runoff amount remains moderately lower than its peak value in August, the October freshwater plume spreads over the entire domain and reaches its maximum (see Fig. 10 of [12]). The river input has a paramount impact on the spatial variability (Fig. 3b) in the sound speed throughout the year except in the pre-monsoon months when the impact is comparatively less. In general, the spatial variability in sound speed is the least in May when the freshwater content is minimal and the temperature throughout the domain remains very high with substantially low spatial variability. This pattern is mostly captured in both simulations and the difference between the spatial fields is minimum. The river impact on the spatial variability (i.e., the difference field) peaks in November. In the absence of the river input, the spatial variability of sound speed in NoRR remains lower than that in RR throughout the year and reaches the minimum (standard deviation ~0.5 m/s) in November. During November, the spatial variability of temperature is minimal, and the river-input-induced freshwater plume causes the salinity variation and hence the sound speed variation. This is how the spatial variation of the surface sound speed is influenced by the river input and its spreading within the Bay due to background circulation.

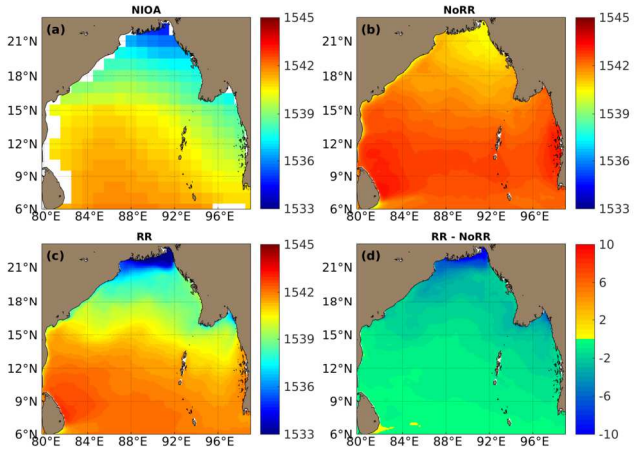

Fig. 2. Spatial maps for the annual mean sound speed from (a) NIOA Climatology, (b) NoRR, (c) RR and (d) difference between RR and NoRR.

Figure 4 presents the spatial maps of the RR and NoRR sound speeds and their differences for May, August, and November representing pre-monsoon, monsoon, and post-monsoon periods. During May the sound speed remained high with minimal spatial variability. The sound speed difference between the two simulations is also very small all over the domain except the coastal areas near the GBM river mouth. During August, the riverine freshwater spreads over the north and eastern parts of the domain and reduces the sound speed in the plume areas. The freshwater plume further extends over a greater/larger extent over a major portion of the domain and reduces the sound speed therein. These findings agree with the seasonal cycles discussed in the previous section.

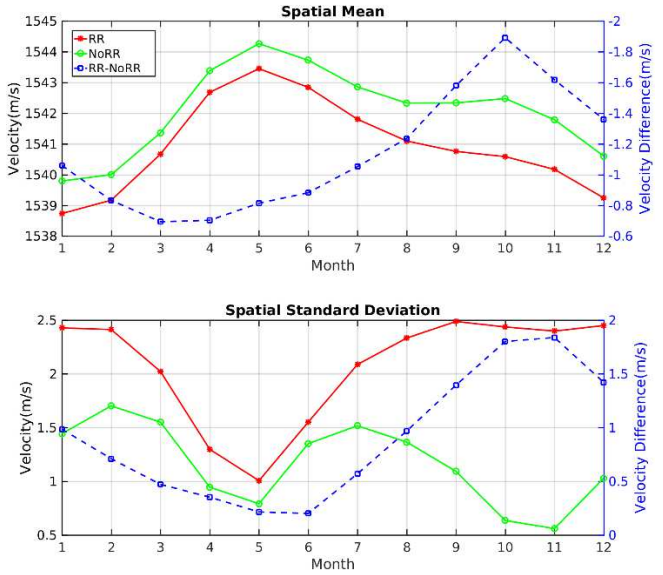

Fig. 3. Seasonal cycle of domain-wide (a) mean and (b) standard deviation of sound speed from RR (red line) and NoRR (green line) runs and their difference (blue dotted line).

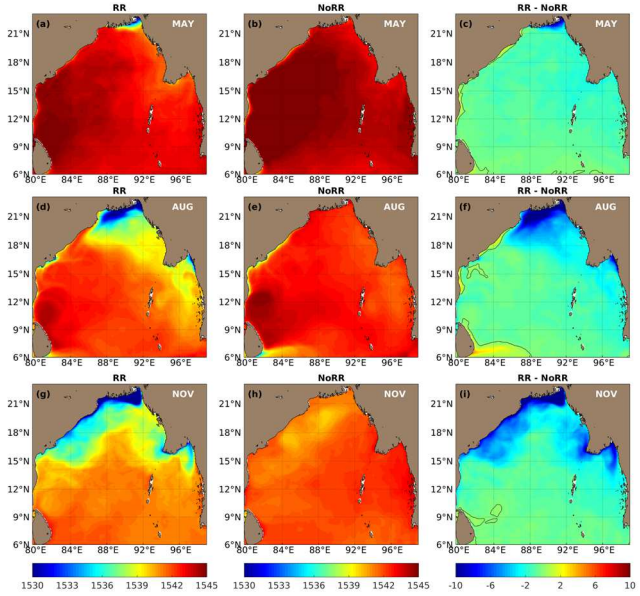

Fig. 4. Sound Speed (m/s) at the surface (a, c) from RR and (b, d) NoRR simulations for May and October. The river impact is minimum in May and maximum in October.

B. *Impact on Vertical Structure and its Variability*

In this section, we present the impact of river input on the vertical structure of the sound speed in the BoB. In the surface layer, the impact of rivers on sound speed mostly occurs due to the salinity change. However, in the subsurface layers, the impact of river input is due to changes in both temperature and

salinity which eventually modulate the sound speed structure. The river impact on salinity gets diluted over depth as the increasing salinity with depth rapidly induces stronger stratification and barrier layer in the northern BoB. This leads to the formation of temperature inversion during the post-monsoon and winter seasons. Such vertically disparate processes in temperature and salinity distribution affect the vertical structure of sound speed. The vertical gradient of sound speed is important as it determines the refraction of sound rays and the formation of sound ducting above the sonic layer depth (SLD) and shadow zone below. The sonic layer depth (SLD) is a crucial parameter in underwater acoustics. It is the depth near the surface where the sound speed is maximum. Within the sonic layer, the vertical gradient of sound speed remains positive, and the sound rays refract upward and can get trapped. As a result, this layer acts as a sound duct, and a shadow zone forms below the SLD. Such surface duct effects also occur in many other ocean regions, e.g. [35], [36].

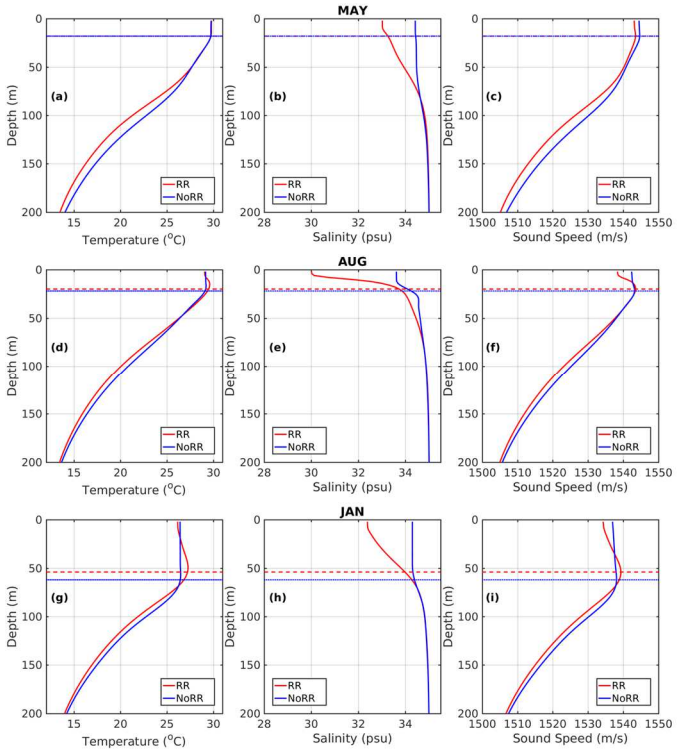

Fig. 5. Vertical profiles of (left column) temperature, (middle column) salinity, (right column) sound speed from RR (red line) and NoRR (blue line) averaged over the box 88-92°E, 18-20°N.The solid red and blue dotted horizontal lines represent the SLDs for RR and NoRR simulations respectively.

As the utmost freshwater impact is observed in the northern BoB, we have selected a box (88-92°E, 18-20°N) there and analyzed the averaged vertical profiles of the sound speed. The box-averaged vertical profiles of temperature, salinity, and sound speed from both simulations for May, August, and January are presented in Fig. 5 (row-wise). It is evident that the vertical structure of the sound speed predominantly follows the pattern of the temperature profile. However, the low saline water in the surface layers reduces the value and enhances the vertical gradient of the sound speed. During May (Fig. 5 - top row), the freshwater impact is minimal, and the weak surface freshening slightly reduces the sound speed of the surface layers. This time, the SLDs in both simulations mostly coincide. During August (Fig. 5 – middle row), the middle of the summer monsoon, the spread of river water and monsoon precipitation results in extensive surface freshening and a strong vertical gradient in salinity leading to the formation of the barrier layer and a weak temperature inversion. The steep salinity gradient, coupled with the temperature inversion substantially enhances the vertical gradient of the sound speed profile as seen in the RR simulation. In the NoRR simulation, the monsoon precipitation alone moderately reduces the surface salinity and hence increases the vertical salinity gradient which results in moderate enhancement in sound speed gradient. Thus, the SLD in the RR simulation is slightly shallower than that in the NoRR simulation. During January (Fig. 5 – bottom row), in the NoRR simulation, the temperature and salinity remain homogeneous within the mixed layer, and the sonic layer forms with a very weak sound speed gradient due to the hydrostatic pressure. On the other hand, during January, the RR simulation exhibits a moderately positive salinity gradient and a firm temperature inversion leading to the formation of a sonic layer with a much stronger positive sound speed gradient which is favorable for strong surface ducting and wider shadow zones. This time, the RR simulation exhibits a shallower SLD than the NoRR. In all these three periods, the colder temperature in RR within the thermocline layer slightly reduces the sound speed in RR compared to NoRR which results in a small increase in the negative vertical gradient in sound speed below the SLD.

IV. Summary and Conclusion

The sound speed structure and its variability play a pivotal role in understanding underwater acoustic propagation and its applications, both in scientific research and strategic endeavors. This variability is intricately linked to the thermohaline conditions within an oceanic region. In the context of the Bay of Bengal (BoB), the thermohaline variability is largely influenced by the influx of freshwater from several major rivers from the adjacent countries. Consequently, it becomes imperative to explore the impact of these river inputs on the sound speed structure within the BoB. However, the challenge arises in that the sound speed estimated from observational data cannot easily distinguish the river impact from other influences. To address this, our study utilizes a high-resolution ROMS modeling system setup to identify the impact of river inputs on the BoB sound speed structure. Two simulations were carried out, one with river inputs and another without. We derived sound speed values from model-simulated temperature and salinity data using Medwin's formula.

We present our findings in terms of how river inputs affect the spatial and temporal variability of sound speed at the surface. In addition, we examined the seasonal variations of the vertical profiles within a defined area in the northern BoB. Our analysis unequivocally demonstrates that river inputs consistently reduce the surface sound speed levels across the domain throughout the year, with the most significant effects observed in the northern areas of the BoB during the post-monsoon period in October. Furthermore, these river inputs significantly enhance the spatial variability of the surface sound speed, peaking in November and reaching its minimum in May.

This spatial variability closely tracks the salinity variability influenced by river inputs.

In the subsurface layers, the impact of river inputs on sound speed manifests itself through changes in both salinity and temperature. As we delve into the subsurface layers, we observe an increase of salinity with depth, leading to a positive gradient that, in turn, intensifies the vertical gradient of sound speed. During the post-monsoon and winter seasons, in addition to the moderate salinity gradient, the presence of temperature inversion significantly enhances the sound speed gradient within the sonic layer, resulting in more pronounced surface ducting. Notably, river inputs lead to a minor cooling in the thermocline, reducing sound speed within this layer while slightly augmenting the vertical gradient of sound speed below the sonic layer depth.

In the future, our findings should be useful for coupled ocean physics and acoustic modeling and forecasting [35]-[41] in the BoB. The effects of rivers should be included in feature models [42] as well as in the extension of satellite and surface data to three dimensions in space [43], [44]. Multiresolution ocean modeling would allow capturing the complex coastal dynamics and submesoscale effects [45] and coupled ocean-weather forecasting systems would enable real-time predictions of river inputs at estuaries [46]. As storms and thus river inputs are uncertain, future studies should also consider probabilistic coupled physical-acoustical forecasting and data assimilation [35], [39], [47], [48]. The new stochastic dynamically-orthogonal acoustic equations could then be employed [49]-[52]. Such probabilistic acoustic predictions could then be utilized to guide autonomous platforms using adaptive sampling toward the most informative location [53]-[57] for capturing the effects of rivers and for efficient ocean monitoring [58],[59]. There are many societal applications in the BoB and its northern regions including sustainable ocean utilization, underwater communication, and marine protection.

ACKNOWLEDGMENT

PFJL and PJH are grateful to the Office of Naval Research for partial support under Grant N00014-19-1-2664 (TFO: DEEP-AI) to the Massachusetts Institute of Technology (MIT). AG acknowledges the support of SMAST/UMassD and the VAJRA award (VJR/2018/000108) from DST, Govt. of India.

REFERENCES

[1] Medwin, H., 1975. Speed of sound in water: A simple equation for realistic parameters. The Journal of the Acoustical Society of America, 58(6),1318-1319.

[2] Chen, C.T. and Millero, F.J., 1977. Speed of sound in seawater at high pressures. The Journal of the Acoustical Society of America, 62(5), 1129-1135.

[3] Fofonoff, N.P. and Millard Jr, R.C., 1983. Algorithms for the computation of fundamental properties of seawater. (Unesco, Paris, France, 1983), 53 pp.

[4] Ali, M.M., Jain, S. and Ramachandran, R., 2011. Effect of temperature and salinity on sound speed in the central Arabian Sea. The open Ocean Engineering Journal, 4(1), 71-76.

[5] Qu, K., Piao, S., Zhou, J. and Zhu, F., 2018. Analysis of surface sound duct in the northern shelf of the south China sea. Shock and Vibration, Article ID 2409761, doi: https://doi.org/10.1155/2018/2409761

[6] S. N. Murty, Y. V. B. Sarma, D. P. Rao, and C. S. Murty, "Water characteristics, mixing and circulation in the Bay of Bengal during southwest monsoon," Journal of Marine Research, vol. 50(2), pp. 207–228, 1992.

[7] Shetye, S. R., 1993. The movement and implications of the Ganges-Brahmaputra runoff on entering the Bay of Bengal, Curr. Sci., 64(1), 32–38.

[8] Han, W., McCreary, J. P.,2001. Modeling salinity distributions in the Indian Ocean.J. Geophys. Res. 106, 859–877.

[9] Han, W., McCreary, J.P., Kohler, K.E., 2001. Influence of precipitation minus evaporation and Bay of Bengal rivers on dynamics, thermodynamics, and mixed layer physics in the upper Indian Ocean. J. Geophys. Res.106(C4), 6895–6916.

[10] Vinayachandran, P. N., and Kurian, J., 2007. Hydrographic observations and model simulation of the Bay of Bengal freshwater plume, Deep Sea Res. I, 54, 471–486.

[11] Benshila, R., Durand, F., Masson, S., Bourdall-Badie, R., de Boyer Montgut, C., Papa, F., Madec, G., 2014. The upper Bay of Bengal salinity structure in a high-resolution model. Ocean Model. 74, 36–52.

[12] Jana, S., Gangopadhyay, A. and Chakraborty, A., 2015. Impact of Seasonal River Input on the Bay of Bengal Simulation. Continental Shelf Research, 104, 45-62

[13] Behara, A., and P. N. Vinayachandran. "An OGCM study of the impact of rain and river water forcing on the Bay of Bengal." Journal of Geophysical Research: Oceans 121, no. 4 (2016): 2425-2446.

[14] Jana, S., Gangopadhyay, A., Lermusiaux, P.F., Chakraborty, A., Sil, S. and Haley Jr., P.J., 2018. Sensitivity of the Bay of Bengal upper ocean to different winds and river input conditions. Journal of Marine Systems, 187, 206-222

[15] Vinayachandran, P. N., Babu, V. R., and Murty, V. S. N., 2002. Observations of barrier layer formation in the Bay of Bengal during summer monsoon, J. Geophys. Res., 107(C12), doi:10.1029/2001JC000831

[16] Thadathil, P., Gopalakrishna, V. V., Muraleedharan, P. M., Reddy, G. V., Araligidad, N., and Shenoy, S., 2002. Surface layer temperature inversion in the Bay of Bengal, Deep Sea Res. I, 49, 1801–1818.

[17] Thadathil, P., Muraleedharan, P. M., Rao, R. R., Somayajulu, Y. K., Reddy, G. V., and Revichandran, C., 2007. Observed seasonal variability of barrier layer in the Bay of Bengal, Journal of Geophysical Research, 112(C02009), doi:10.1029/2006JC003651.

[18] Girishkumar, M. S., M. Ravichandran, and M. J. McPhaden. "Temperature inversions and their influence on the mixed layer heat budget during the winters of 2006–2007 and 2007–2008 in the Bay of Bengal." Journal of Geophysical Research: Oceans 118, no. 5 (2013): 2426-2437.

[19] Kumar, S.P., Navelkar, G.S., Murty, T.V., Somayajulu, Y.K. and Murty, C.S., 1993. Sound speed structure in the Arabian Sea and the Bay of Bengal, Indian Journal of Marine Sciences, 22(1), 17 – 20.

[20] Navelkar, G.S., Somayajulu, Y.K. and Murty, C.S., 1996. Sound field computations in the Bay of Bengal using parabolic equation method. Indian Journal of Marine Sciences, 25(179-183)

[21] Hareesh Kumar, P.V., 2013. The sound channel characteristics in the south central Bay of Bengal. International Journal of Innovative Technology and Exploring Engineering, 3, pp.61-5.

[22] Zacharia, Shijo, R. Seshasayanan, Tata Sudhakar, M. A. Atmanand, and R. R. Rao. "Observed variability of surface layer in the Central Bay of Bengal: results of measurements using glider." Current Science (2017): 2151-2159

[23] Sinha, S.K., Dewangan, P. and Sain, K., 2016. Acoustic reflections in the water column of Krishna-Godavari offshore basin, Bay of Bengal. The Journal of the Acoustical Society of America, 139(5), pp.2424-2431.

[24] Jana, S., Gangopadhyay, A., Haley, P.J. and Lermusiaux, P.F.J., 2022, February. Sound Speed Variability over Bay of Bengal from Argo Observations (2011-2020). In OCEANS 2022-Chennai (pp. 1-8). IEEE. DOI: 10.1109/OCEANSChennai45887.2022.9775509

[25] Haidvogel, D. B., Arango, H. G., Hedstrom, K., Beckmann, A., Malanotte-Rizzoli, P., & Shchepetkin, A. F. (2000). Model evaluation experiments in the North Atlantic Basin: simulations in nonlinear terrain-following coordinates. Dynamics of atmospheres and oceans, 32(3-4), 239-281.

[26] Shchepetkin, A. F., McWilliams, J. C., 2003. A method for computing horizontal pressure-gradient force in an oceanic model with a nonaligned vertical coordinate. Journal of Geophysical Research: Oceans, 108(C3).

[27] Shchepetkin, A.F. and McWilliams, J.C., 2005. The regional oceanic modeling system (ROMS): a split-explicit, free-surface, topography-following-coordinate oceanic model. Ocean modelling, 9(4), pp.347-404.

[28] Risien, C.M. and Chelton, D.B., 2008. A global climatology of surface wind and wind stress fields from eight years of QuikSCAT scatterometer data. Journal of Physical Oceanography, 38(11),.2379-2413.

[29] Yu, L., Weller, R.A., 2007. Objectively analyzed air–sea heat fluxes for the global ice-free oceans (1981–2005). Bull. Am. Meteorol. Soc. 88, 527–539.

[30] Yu, L., Jin, X., Weller, R.A., 2008. Multidecade Global Flux Datasets from the Objectively Analyzed Air–Sea Fluxes (OAFlux) Project: Latent and Sensible Heat Fluxes, Ocean Evaporation, and Related Surface Meteorological Variables. Woods Hole

[31] Yeager, S.G., Large, W.G., 2008. CORE.2 global air–sea flux dataset. In: Research Data Archive at the National Center for Atmospheric Research. Computational and Information Systems Laboratory. https://doi.org/10.5065/D6WH2N0S.

[32] da Silva, A.M., Young, C.C., Levitus, S., 1994. Atlas of surface marine data 1994. Algorithms and Procedures. vol. 1 NOAA Atlas NESDIS 6, U.S. Department of Commerce, NOAA, NESDIS.

[33] Fairall, C.W., Bradley, E.F., Rogers, D.P., Edson, J.B. and Young, G.S., 1996. Bulk parameterization of air-sea fluxes for tropical ocean-global atmosphere coupled-ocean atmosphere response experiment. Journal of Geophysical Research: Oceans, 101(C2),.3747-3764.

[34] Chatterjee, A., Shankar, D., Shenoi, S.S.C., Reddy, G.V., Michael, G.S., Ravichandran, M., Gopalkrishna, V.V., Rama Rao, E.P., Udaya Bhaskar, T.V.S. and Sanjeevan, V.N., 2012. A new atlas of temperature and salinity for the North Indian Ocean. Journal of Earth System Science, 121, 559-593.

[35] Lermusiaux, P.F.J., P.J. Haley, Jr., C. Mirabito, W.H. Ali, M. Bhabra, P. Abbot, C.-S. Chiu, and C. Emerson, 2020a. Multi-resolution Probabilistic Ocean Physics-Acoustic Modeling: Validation in the New Jersey Continental Shelf. In: OCEANS '20 IEEE/MTS, 5-30 October 2020, pp. 1-9. doi:10.1109/IEEECONF38699.2020.9389193

[36] Ali, W.H., A. Charous, C. Mirabito, P.J. Haley, Jr., and P.F.J. Lermusiaux, 2023. MSEAS-ParEq for Ocean-Acoustic Modeling around the Globe. In: OCEANS '23 IEEE/MTS Gulf Coast, 25–28 September 2023. doi:10.23919/OCEANS52994.2023.10337377

[37] Lam, F.P, P.J. Haley, Jr., J. Janmaat, P.F.J. Lermusiaux, W.G. Leslie, and M.W. Schouten, 2009. At-sea Real-time Coupled Four-dimensional Oceanographic and Acoustic Forecasts during Battlespace Preparation 2007. Special issue of the Journal of Marine Systems on "Coastal processes: challenges for monitoring and prediction", Drs. J.W. Book, Prof. M. Orlic and Michel Rixen (Guest Eds.), 78, S306-S320, doi: 10.1016/j.jmarsys.2009.01.029.

[38] P. F. J. Lermusiaux, J. Xu, C. F. Chen, S. Jan, L. Y. Chiu, and Y. J. Yang, 2010. "Coupled ocean–acoustic prediction of transmission loss in a continental shelfbreak region: Predictive skill, uncertainty quantification, and dynamical sensitivities," IEEE Journal of Oceanic Engineering, vol. 35, no. 4, pp. 895-916.

[39] Lermusiaux, P.F.J., C. Mirabito, P.J. Haley, Jr., W.H. Ali, A. Gupta, S. Jana, E. Dorfman, A. Laferriere, A. Kofford, G. Shepard, M. Goldsmith, K. Heaney, E. Coelho, J. Boyle, J. Murray, L. Freitag, and A. Morozov, 2020b. Real-time Probabilistic Coupled Ocean Physics-Acoustics Forecasting and Data Assimilation for Underwater GPS. In: OCEANS '20 IEEE/MTS, 5-30 October 2020, pp. 1-9. doi:10.1109/IEEECONF38699.2020.9389003.

[40] Duda, T.F., Y.-T. Lin, A.E. Newhall, K.R. Helfrich, W.G. Zhang, M. Badiey, P.F.J. Lermusiaux, J.A. Colosi, and J.F. Lynch, 2014. The "Integrated Ocean Dynamics and Acoustics" (IODA) Hybrid Modeling Effort, Proceedings of the international conference on Underwater Acoustics - 2014 (UA2014), 621-628.

[41] Duda, Timothy F., Ying-Tsong Lin, Arthur E. Newhall, Karl R. Helfrich, James F. Lynch, Weifeng Gordon Zhang, Pierre FJ Lermusiaux, and John Wilkin. "Multiscale multiphysics data-informed modeling for three-dimensional ocean acoustic simulation and prediction." The Journal of the Acoustical Society of America 146, no. 3 (2019): 1996-2015.

[42] Gangopadhyay, A., P.F.J. Lermusiaux, L. Rosenfeld, A.R. Robinson, L. Calado, H.S. Kim, W.G. Leslie and P.J. Haley, Jr., 2011. The California Current System: A Multiscale Overview and the Development of a Feature-Oriented Regional Modeling System (FORMS). Dynamics of Atmospheres and Oceans, 52, 131-169, doi:10.1016/j.dynatmoce.2011.04.003.

[43] Lermusiaux, P.F.J., D.G.M. Anderson and C.J. Lozano, 2000. On the mapping of multivariate geophysical fields: error and variability subspace estimates. The Quarterly Journal of the Royal Meteorological Society, April B, 1387-1430.

[44] Lin, Y.-T., A.E. Newhall, T.F. Duda, P.F. J. Lermusiaux and P.J. Haley, Jr., 2010. Merging Multiple Partial-Depth Data Time Series Using Objective Empirical Orthogonal Function Fitting. IEEE Transactions, Journal of Oceanic Engineering. 35(4) 710-721. doi:10.1109/JOE.2010.2052875.

[45] Deleersnijder, E., V. Legat and P.F.J. Lermusiaux, 2010. Multi-scale modelling of coastal, shelf and global ocean dynamics. Ocean Dynamics. 60, 1357-1359. doi:10.1007/s10236-010-0363-6

[46] Hoteit, I., Y. Abualnaja, S. Afzal, B. Ait-El-Fquih, T. Akylas, C. Antony, C. Dawson, K. Asfahani, R.J. Brewin, L. Cavaleri, I. Cerovecki, B. Cornuelle, S. Desamsetti, R. Attada, H. Dasari, J. Sanchez-Garrido, L. Genevier, M. El Gharamti, J.A. Gittings, E. Gokul, G. Gopalakrishnan, D. Guo, B. Hadri, M. Hadwiger, M.A. Hammoud, M. Hendershott, M. Hittawe, A. Karumuri, O. Knio, A. Köhl, S. Kortas, G. Krokos, R. Kunchala, L. Issa, I. Lakkis, S. Langodan, P. Lermusiaux, T. Luong, J. Ma, O. Le Maitre, M. Mazloff, S. El Mohtar, V.P. Papadopoulos, T. Platt, L. Pratt, N. Raboudi, M.-F. Racault, D.E. Raitsos, S. Razak, S. Sanikommu, S. Sathyendranath, S. Sofianos, A. Subramanian, R. Sun, E. Titi, H. Toye, G. Triantafyllou, K. Tsiaras, P. Vasou, Y. Viswanadhapalli, Y. Wang, F. Yao, P. Zhan, and G. Zodiatis, 2021. Towards an End-to-End Analysis and Prediction System for Weather, Climate, and Marine Applications in the Red Sea. Bulletin of the American Meteorological Society 102(1), E99-E122. doi:10.1175/BAMS-D-19-0005.1

[47] Lermusiaux, P.F.J., 2006. Uncertainty Estimation and Prediction for Interdisciplinary Ocean Dynamics. Refereed manuscript, Special issue on "Uncertainty Quantification". J. Glimm and G. Karniadakis, Eds. Journal of Computational Physics, 217, 176-199. doi: 10.1016/j.jcp.2006.02.010

[48] Evangelinos, C., P.F.J. Lermusiaux, J. Xu, P.J. Haley, and C.N. Hill, 2011. Many Task Computing for Real-Time Uncertainty Prediction and Data Assimilation in the Ocean. IEEE Transactions on Parallel and Distributed Systems, Special Issue on Many-Task Computing, I. Foster, I. Raicu and Y. Zhao (Guest Eds.), 22, doi: 10.1109/TPDS.2011.64

[49] Ali, W.H., M.S. Bhabra, P.F.J. Lermusiaux, A. March, J.R. Edwards, K. Rimpau, and P. Ryu, 2019. Stochastic Oceanographic-Acoustic Prediction and Bayesian Inversion for Wide Area Ocean Floor Mapping. In: OCEANS '19 MTS/IEEE Seattle, 27-31 October 2019, doi:10.23919/OCEANS40490.2019.8962870

[50] Charous, A. and P.F.J. Lermusiaux, 2021. Dynamically Orthogonal Differential Equations for Stochastic and Deterministic Reduced-Order Modeling of Ocean Acoustic Wave Propagation. In: OCEANS '21 IEEE/MTS San Diego, 20-23 September 2021, pp. 1-7, in press.

[51] Ali, W.H., and P.F.J. Lermusiaux, 2024a. Dynamically Orthogonal Narrow-Angle Parabolic Equations for Stochastic Underwater Sound Propagation. Part I: Theory and Schemes. Journal of the Acoustical Society of America 155(1), 640-655. doi:10.1121/10.0024466

[52] Ali, W.H., and P.F.J. Lermusiaux, 2024b. Dynamically Orthogonal Narrow-Angle Parabolic Equations for Stochastic Underwater Sound Propagation. Part II: Applications. Journal of the Acoustical Society of America 155(1), 656-672. doi:10.1121/10.0024474

[53] Wang, D., P.F.J. Lermusiaux, P.J. Haley, D. Eickstedt, W.G. Leslie and H. Schmidt, 2009. Acoustically Focused Adaptive Sampling and On-board Routing for Marine Rapid Environmental Assessment. Special issue of Journal of Marine Systems on "Coastal processes: challenges for monitoring and prediction", Drs. J.W. Book, Prof. M. Orlic and Michel Rixen (Guest Eds), 78, S393-S407, doi: 10.1016/j.jmarsys.2009.01.037

[54] Schofield, O., S. Glenn, J. Orcutt, M. Arrott, M. Meisinger, A. Gangopadhyay, W. Brown, R. Signell, M. Moline, Y. Chao, S. Chien, D. Thompson, A. Balasuriya, P.F.J. Lermusiaux and M. Oliver, 2010. Automated Sensor Networks to Advance Ocean Science. EOS, Vol. 91, No. 39, 28 September 2010

[55] Centurioni, L.R., V. Hormann, L. D. Talley, I. Arzeno, L. Beal, M. Caruso, P. Conry, R. Echols, H. J. S. Fernando, S. N. Giddings, A. Gordon, H. Graber, R. Harcourt, S. R. Jayne, T. G. Jensen, C. M. Lee, P. F. J. Lermusiaux, P. L'Hegaret, A. J. Lucas, A. Mahadevan, J. L. McClean, G. Pawlak, L. Rainville, S. Riser, H. Seo, A. Y. Shcherbina, E. Skyllingstad, J. Sprintall, B. Subrahmanyam, E. Terrill, R. E. Todd, C. Trott, H. N. Ulloa, and H. Wang, 2017. Northern Arabian Sea Circulation-Autonomous Research (NASCar): A Research Initiative Based on Autonomous Sensors. Oceanography 30(2):74–87, https://doi.org/10.5670/oceanog.2017.224

[56] Lermusiaux, P.F.J., P.J. Haley Jr., S. Jana, A. Gupta, C.S. Kulkarni, C. Mirabito, W.H. Ali, D.N. Subramani, A. Dutt, J. Lin, A. Y. Shcherbina, C. M. Lee, and A. Gangopadhyay, 2017a. Optimal Planning and Sampling Predictions for Autonomous and Lagrangian Platforms and Sensors in the Northern Arabian Sea. Oceanography 30(2):172–185, https://doi.org/10.5670/oceanog.2017.242.

[57] Lermusiaux, P.F.J., D.N. Subramani, J. Lin, C.S. Kulkarni, A. Gupta, A. Dutt, T. Lolla, P.J. Haley Jr., W.H. Ali, C. Mirabito, and S. Jana, 2017b. A Future for Intelligent Autonomous Ocean Observing Systems. The Sea. Volume 17, The Science of Ocean Prediction, Part 2, J. Marine Res. 75(6), pp. 765–813. https://doi.org/10.1357/002224017823524035

[58] Lermusiaux, P.F.J., P.J. Haley Jr. and N.K. Yilmaz, 2007. Environmental Prediction, Path Planning and Adaptive Sampling: Sensing and Modeling for Efficient Ocean Monitoring, Management and Pollution Control. Sea Technology, 48(9), 35-38.

[59] Tieppo, M., E. Pereira, L. González Garcia, M. Rolim, E. Castanho, A. Matos, A. Silva, B. Ferreira, M. Pascoal, E. Almeida, F. Costa, F. Zabel, J. Faria, J. Azevedo, J. Alves, J. Moutinho, L. Gonçalves, M. Martins, N. Cruz, N. Abreu, P. Silva, R. Viegas, S. Jesus, T. Chen, T. Miranda, A. Papalia, D. Hart, J. Leonard, M. Haji, O. de Weck, P. Godart, and P. F.J. Lermusiaux, 2022. Submarine Cables as Precursors of Persistent Systems for Large Scale Oceans Monitoring and Autonomous Underwater Vehicles Operation. In: OCEANS '22 IEEE/MTS Hampton Roads, 17–20 October 2022, pp. 1–7. doi:10.1109/OCEANS47191.2022.997